LWT - Food Science and Technology 171 (2022) 114128

Contents lists available at ScienceDirect

LWT

journal homepage: www.elsevier.com/locate/lwt

Influence of pork liver drying on ferrochelatase activity for zinc protoporphyrin formation

B. Abril [a], E.A. Sanchez-Torres [a], R. Bou [b], J. Benedito [a], Jose V. Garcia-Perez [a,*]

[a] Department of Food Technology, Universitat Politècnica de València, Camí de Vera, s/n, 46022, Valencia, Spain
[b] Food Safety and Functionality Program, Institut de Recerca i Tecnologia Agroalimenntàries (IRTA), Finca Camps i Armet s/n, 17121, Monells, Girona, Spain

ARTICLE INFO

Keywords:
Ferrochelatase
Zinc protoporphyrin
Drying
Pork liver
Coproduct
Revalorisation

ABSTRACT

Pork liver contains an endogenous enzyme, ferrochelatase (FeCH), which catalyses the formation of zinc protoporphyrin (ZnPP), a natural pigment of great interest for the meat industry. The aim of this study was to analyse the effect of pork liver drying (from −10 to 70 °C), as a stabilisation method, on the FeCH activity (EA) and the apparent concentration (EC_{app}). Drying temperatures close to room conditions (from 10 to 20 °C) allowed to preserve well the EC_{app}, while the EA was slightly lower (−15.2%) than in raw liver. However, when drying was conducted at extreme conditions (−10 and 70 °C), the lowest values of EC_{app} and EA were manifested. Therefore, the drying process at moderate temperatures close to room conditions (10 - 20 °C) was considered to be an effective method for FeCH preservation since it was possible to stabilise the liver and the loss of FeCH activity was minimised.

1. Introduction

Currently, there is increasing demand for natural ingredients, thereby avoiding the use of chemicals in the food industry. In this context, zinc protoporphyrin (ZnPP) could be considered a natural ingredient with noticeable technological properties. ZnPP is a compound found in red blood cells, similar to the heme group, except that the iron atom (Fe) of the porphyrin ring has been replaced by a zinc atom (Zn). Furthermore, unlike the heme group, the ZnPP complex exhibits a high level of fluorescence and is easily detectable in small amounts. ZnPP is of great technological interest due to its reddish colour and its high degree of light and thermal stability (Adamsen et al., 2004; Morita et al., 1996). Wakamatsu, Nishimura, and Hattori (2004) postulated the ZnPP formation in Parma ham, this compound being responsible for the characteristic purple-red colour of this type of ham, which is manufactured using neither nitrates nor nitrites. Therefore, the use of ZnPP as a colorant for the purposes of improving the colour of meat products, both dry-cured and cooked, is of great interest at industrial level.

The ZnPP formation is catalysed by the enzyme ferrochelatase (FeCH), which facilitates the replacement of the Fe atom, present in the heme group, by the Zn atom (Chau et al., 2010, 2011). Taketani and Tokunaga (1982) found that the FeCH could be extracted from the bovine liver to obtain ZnPP. In addition, subsequent studies demonstrated that one of the most interesting sources of FeCH, from which it is possible to obtain the ZnPP pigment, was pork liver (Wakamatsu et al., 2015). Nowadays, pork liver is a co-product of the meat industry; it is of low commercial value and is mainly used for the production of pâtés and animal feed (Estévez et al., 2004). In slaughterhouses, large quantities of co-products and residues, such as liver, heart, kidney, skin, blood or bones, are generated. Every year, around 330 million animals (cows, sheep, pigs and goats) are slaughtered in the EU, which generates more than 17 million tons of meat co-products (EFPRA, 2021). The management of co-products, as well as the elimination of waste from the meat industry, is becoming a serious concern, contributing to environmental pollution. For this reason, it is necessary to seek new uses for meat co-products that allow their revaluation, thus contributing to the concept of circular economy (Echegaray et al., 2018). In this context, pork liver extracts with a high degree of FeCH activity are postulated as potential food ingredients for the meat industry, due to their ability to catalyse ZnPP formation (Abril et al., 2021). However, liver is a perishable product due to its large amount of water and heavy microbial load. Consequently, drying represents a necessary stage in the stabilisation of pork liver in order to prolong its shelf life at a moderate cost. This would facilitate both the FeCH extraction and the subsequent valorisation of the protein fraction.

Convective drying, using forced air, is the most popular dehydration

* Corresponding author.
E-mail address: jogarpe4@tal.upv.es (J.V. Garcia-Perez).

https://doi.org/10.1016/j.lwt.2022.114128
Received 5 July 2022; Received in revised form 20 October 2022; Accepted 26 October 2022
Available online 27 October 2022

technique in the food industry. During drying, the moisture is removed by evaporation or sublimation, depending on the process temperature (Santacatalina et al., 2011). Sanchez-Torres et al. (2021) recently reported the sorption isotherms of pork liver, which are essential for the optimal design of its drying process, allowing the subsequent extraction of enzymes or protein fractions. Drying reduces the water availability for enzymatic and microbial degradation (Baque, Macías, & Cornejo, 2010). However, drying may affect the structure and activity of food enzymes (Oyinloye & Yoon, 2020). Enzyme degradation will depend on the stress caused during drying, which is mainly dependent on the drying temperature and time. Temperature is a key factor for enzymes since, in some cases, they maintain their activity at temperatures below 4 °C (known as cold-adapted enzymes), while other enzymes are active at temperatures above 95 °C (known as thermostable enzymes) (Kuddus, 2019). On the one hand, heat exposure may reduce the enzymatic activity due to the denaturation of the protein structure (Guiné, 2018). Thus, Perdana et al. (2012) carried out a study into the influence of drying on the β-galactosidase enzyme in the maltodextrin matrix, observing that the enzymes are heat sensitive and, therefore, can be partially or completely inactivated during drying, depending on the temperature applied. These authors observed that the β-galactosidase inactivation is more intense (inactivation rate 0.001 mol s^{-1}) at the beginning of drying and reported a reduction of only 3% in the enzymatic activity caused by spray drying. On the other hand, drying at low temperatures may also cause a decrease in the enzyme activity (Roy & Gupta, 2004) due to the fact that this type of drying involves lengthy exposure to the stress characteristic. Thus, Parra Vergara (2013) observed a significant decrease in the activity of the peroxidase enzyme in lyophilised broccoli (10.50% residual peroxidase enzyme activity, UPOD) compared to the fresh broccoli. In this context, an analysis of the effect of temperature on pork liver drying, as a pre-treatment to the further FeCH extraction, would help us gain insight not only into the drying process, but also into the impact on the activity of the extracted enzyme. In this regard, there have been no previous references addressing the drying of pork liver or other meat co-products for further enzyme extraction over a wide temperature range. Therefore, the objective of this study was to assess the impact of temperature (from −10 to 70 °C) on the drying kinetics of liver and the FeCH activity for ZnPP formation obtained from the dehydrated product.

2. Materials and methods

2.1. Raw materials and sample preparation

Raw pork livers were obtained from the slaughterhouse “Carnes de Teruel S.A.” (D.O. Jamón de Teruel, Spain) and transported to the laboratory in refrigeration (4 ± 2 °C). The initial preparation of the pork liver firstly consisted of the separation of its 4 main lobes: the right lateral, left lateral, right medial and left medial. Secondly, each lobe was divided into 2 parts, and all the obtained parts were vacuum packaged (200 × 300 PA/PE, Sacoliva, Castellar del Vallès, Barcelona), labelled with a number corresponding to the liver and the lobe and stored at −20 °C until used in the drying experiments. For each drying experiment, 2 parts were taken out of the freezer (−20 °C), avoiding taking parts from the same liver and kept in refrigeration (4 ± 2 °C) for 2 h before use. Afterwards, cylindrical samples (15 mm in height and 12.6 mm in diameter) were obtained using a household tool and the remaining part of the liver was homogenised and used to determine the initial moisture content and FeCH activity, as explained in sections 2.5 and 2.6. For each drying process, 20 cylindrical samples were placed into a custom sample holder inside the drying chamber, weighing 43 ± 0.5 g.

2.2. Determination of moisture content

The moisture content was determined using the AOAC method n° 940.44 (AOAC, 1997). Approximately 3 g of liver were homogenised by grinding (Manta BL201, 200W, Spain). Then, 2 g of sand were mixed with 3 g of the sample and placed into a convective oven (ED 115, Binder Gmbh, Alemania) at 105 °C for 24 h. Afterwards, the samples were placed into a desiccator for tempering before weighing. The moisture content was determined in triplicate for each experimental run.

2.3. Convective drying at low and high temperatures

The two types of convective drying processes were defined from the standard room conditions (20 °C) (Santacatalina et al., 2014). Low temperature drying was carried out at temperatures equal to or lower than the standard room conditions (20, 10, 0 and −10 °C) whereas high temperature drying was carried out at temperatures above the standard room conditions (30, 40, 50, 60 and 70 °C).

The drying experiments were carried out in two different convective driers with temperature and air velocity control, which have already been described in the literature (García-Pérez et al., 2011; García-Pérez et al., 2012). The weight of the sample was automatically measured and recorded at regular time intervals. High temperature drying experiments were carried out in the drying chamber, which was made up of an aluminium cylinder (internal diameter 10 cm, height 31 cm, and thickness 1 cm) where the sample holder was located. The heating set-up consisted of a ventilation system, which had a medium pressure centrifugal fan (COT-100, Soler & Palau, Spain) that drove the drying air into the drying chamber, previous to which it had passed through the heating resistors controlled by a PID algorithm from a PLC (PLC CQM41, OMRON, Japan). Air velocity (2 ± 0.1 m/s) was measured by a winged wheel anemometer (1468, Wilh, Lambrecht GmbH, Germany).

As regards low temperature drying, the experiments were carried out in a drying chamber comprised of an aluminium cylinder (internal diameter 10 cm, height 31 cm, and thickness 1 cm) inside which the cylindrical liver samples were placed in the sample holder. A centrifugal fan (COT-100, Soler & Palau, Spain) was in charge of driving the air flow through the drying chamber and the air velocity was measured with an anemometer (1468, Wilh. Lambrecht Gmbh, Germany). The airflow was controlled by a PLC (cFP-2220, National Instruments, USA) using a PID algorithm and acting on a frequency inverter (MX2, Omron, Japan). The air temperature was modified by combining a heat exchanger and electric resistors. The airflow was cooled down as it passed through the heat exchanger (area 13 m^2, fin space 9 mm; Frimetal, Spain) which was connected to refrigeration equipment and, subsequently, the electrical resistors adjusted the desired temperature using a PID algorithm. The relative humidity of the drying air was kept below 15% by passing the airflow through a set of trays with a bed of desiccant material (drying bead height 1.5 cm, particle size 6–8 mm, Rung Rueng Cosulting, Thailand). The trays were periodically refilled with new desiccant material regenerated in an oven at 150 °C (ED 115, Binder Gmbh, Germany).

The drying experiments were conducted in triplicate and completed when the samples lost 70% of their initial weight. Subsequently, they were ground and the final moisture content was determined. Finally, the samples were vacuum packed and stored at 4 ± 2 °C until the enzymatic activity was measured.

2.4. Drying kinetics and mathematical model fitting

Mathematical modelling of the drying kinetics is necessary to assess the influence of the drying temperature and predict the behaviour of the material under different process conditions. The empirical Weibull model was used to compute the influence of the temperature on the drying time. Equation (1) illustrates the probabilistic distribution of Weibull used to describe the evolution of moisture during drying (Cunha et al., 1998).

$$Wt = We + (W0 - We) \cdot \exp\left[-\left(\frac{t}{\beta}\right)\right]^{\alpha} \quad \text{(Equation 1)}$$

where W_t is the average moisture content (kg water/kg dry matter) at time t (s), W_e is the equilibrium moisture content (kg water/kg dry matter) and W_0 is the initial moisture content (kg water/kg dry matter). As for the Weibull distribution model, β is the kinetic parameter (s), having an inverse relationship with the drying rate; that is, the higher the β, the slower the process. α, meanwhile, is the shape parameter, reflecting the behaviour of the sample during drying (Cunha et al., 1998). The shape parameter is related to the velocity of the mass transfer at the beginning; thus, the lower the α value, the faster the initial drying rate (Buzrul, 2022). If $\alpha > 1$, this indicates an initial delay in the drying process and $\alpha = 1$ means that the model presents a first order kinetics.

The parameters of the Weibull model were identified by minimising the sum of the squared differences between the experimental and calculated moisture using the Solver Microsoft Excel™ tool, available in the Microsoft Excel spreadsheet, which uses the Generalised Reduced Gradient optimisation method (GRG) (García-Pérez, 2007). The percentages of the mean relative error (%MRE, Equation (2)) and explained variance (%VAR, Equation (3)) were computed to assess the goodness of the fit.

$$\%MRE = \frac{100}{N}\left[\sum_{i=1}^{N}\frac{|W\,exp - Wcal|}{Wexp}\right] \quad \text{(Equation 2)}$$

$$\%VAR = \left[1 - \frac{Sxy^2}{Sy^2}\right]\cdot 100 \quad \text{(Equation 3)}$$

where W_{exp} and W_{cal} are the experimental and the estimated moisture, respectively; N is the number of experimental data and S_{xy} and S_y are the standard deviations of the estimation and the sample deviation, respectively.

From simulated drying kinetics at the different temperatures, the drying time required to reach a moisture content of 0.10 kg water/kg dry matter (70% loss of the initial weight) was computed using the identified Weibull parameters in order to better compare the influence of the temperature. This approach minimises the experimental error of computing the drying time from experimental data. The kinetic parameter of the Weibull model (inverse of β) presents an Arrhenius-type relationship with the temperature (Meziane, 2011), as shown by Equation (4).

$$\frac{1}{\beta} = \frac{1}{\beta 0}\exp\left(\frac{-Ea}{RT}\right) \quad \text{(Equation 4)}$$

where $1/\beta_0$ (s^{-1}) is the pre-exponential factor, E_a (kJ/mol) the activation energy, R (kJ/mol·K) the universal gas constant and T (K) the drying temperature.

2.5. Ferrochelatase extraction

The Ferrochelatase (FeCH) enzyme was extracted from raw pork liver following the methodology proposed by Abril *et al.* (2021), whereas some minor modifications in this methodology were introduced when FeCH was extracted from the dried liver due to the moisture reconstitution. Firstly, 3 g of dried pork liver was ground (Blixer 2, Robot Coupe USA, Inc., Jackson Ms, USA). Secondly, the ground dried pork liver was rehydrated with distilled water (0.7 g of water per 0.3 g of dried liver) until it reached its initial moisture content. Thus, 1 g of raw or reconstituted dried liver was homogenised (Homogeniser DI 25 Basic, IKA, Germany) with 25 mL of extraction buffer at 4 °C for 1 min, at 8000 rpm, using a 50 mL glass beaker. The extraction buffer was made up of 50 mM Tris-HCl, 20% Glycerol (w/v), 0.8% KCl (w/v) and 1% Triton X-100 (w/v) (Sigma Aldrich) and was adjusted to pH = 8 with NaOH. Secondly, FeCH extraction was carried out by stirring for 30 min using a magnetic stirrer (SM3, STUART, UK). Subsequently, the FeCH extract was kept at 4 ± 2 °C in order to avoid modifications in the enzyme. Finally, in order to separate the enzyme fraction, the sample was centrifuged for 10 min at 12500 rpm and at 4 °C (Medifriger BL-S, SELECTA, Spain), and then the obtained supernatant was filtered (Whatman 597, GE LIFE SCIENCE, United States). This fraction containing the FeCH was used as the enzyme source in the formation kinetics of ZnPP.

2.6. Zinc-protoporphyrin formation kinetics

ZnPP formation kinetics were carried out following the experimental method described by Abril et al. (2021). The enzymatic reaction was produced in microtubes of 2 mL, incubated at 37 ± 0.5 °C in a water bath. Thus, the FeCH fraction obtained from the liver extract (300 μL) was mixed with the two substrates: Zinc (250 μL $ZnSO_4$ in Tris-HCl buffer, adjusted to pH = 8.0), and the protoporphyrin source (50 μL Protoporphyrin IX in Tris-HCl buffer, adjusted to pH = 7.0). In addition, ATP (200 μL of ATP solution in 20% NaCl, w/v) was also added to the mixture. Blank samples were used to detect any background fluorometric signal from the reagents and were prepared by adding all the reagents except the 300 μL of the FeCH fraction (liver extract).

The microtubes were incubated at different times (0, 15, 30, 45, 60, 90, 105, 120 min) to determine the reaction kinetics of ZnPP formation. The enzymatic reaction was stopped by adding 35 μL of EDTA and 840 μL of cold absolute ethanol. Then, the samples were centrifugated for 30 min at 13200 rpm and 4 °C (5415R, EPPENDORF, Germany) and, subsequently, the obtained supernatant was measured by fluorescence (200 μL). Fluorescent analyses were carried out as described by Wakamatsu, Okui, et al. (2004), with minor modifications. The fluorescence spectrum of ZnPP was measured from 420 to 590 nm for the purposes of excitation using a spectrofluorophotometer with an 96-well plate (Infinite 200 Microplate Reader, TECAN, Switzerland). In order to determine the concentration of ZnPP (μM), the calibration curve reported by Abril et al. (2021) was considered. ZnPP formation kinetic was carried out in triplicate for pork liver dried at the different temperatures, while it was also performed using the remaining raw pork liver in each drying run.

Abril et al. (2021) defined the enzyme activity, expressed in terms of the product formation rate, as the derivative of ZnPP concentration with time, as shown in Equation (5).

$$EA = \frac{dP}{dt} \quad \text{(Equation 5)}$$

where EA is the enzyme activity (μM/min), P the ZnPP concentration (μM), and t the time (min).

Abril et al. (2021) observed two phases in the kinetics of ZnPP formation: i) an initial burst phase during the first 15 min followed by ii) a steady rate phase. The burst phase indicates an initial stage in the enzyme reaction which occurs at a very high rate, related to the first turnover of the active sites (Praestgaard et al., 2011). Afterwards, the enzyme reaction enters the steady state phase in which a constant reaction rate is manifested, coinciding with the slope of the linear relationship and computing the enzyme activity (EA). Meanwhile, the y-intercept would represent the ZnPP concentration formed during the first turnover of the enzyme, being directly proportional to the active enzyme concentration and possibly postulated as an apparent-FeCH concentration (EC_{app}, μM) (Sassa et al., 2013).

2.7. Statistical analysis

The influence of the drying temperature on the FeCH concentration and enzyme activity was statistically evaluated by analysis of variance (ANOVA). Fisher's least significant difference (LSD) procedure was used to identify the differences between the averages with a confidence

interval of 95% ($p < 0.05$). The Statistical analysis was performed by using Centurion XVI software (Statpoint Technologies Inc., Warrenton, VA, USA).

3. Results and discussion

3.1. Drying of pork liver at different temperatures

In order to evaluate the influence of air temperature on drying kinetics, experiments were carried out at temperatures ranging from −10 to 70 °C. As stated in Section 2.4., an experimental moisture content of 0.10 kg water/kg dry matter (70% loss of the initial weight) was set to determine the drying time. The results obtained for the experiments showed that the air temperature affected the drying kinetics, shortening the drying time (Figs. 1A and 2A). Thus, the drying times necessary to achieve a 70% loss in the initial weight ranged between 838.8 h at −10 °C and 12.1 h at 70 °C (Table 1). This large time difference can be explained if we consider that, the water changes from a solid to a vapour state in the atmospheric drying experiment (−10 °C), a phenomenon known as sublimation, and further diffusion of the vapour through the drying solid occurs at very low temperatures (García-Pérez et al., 2012). However, in the case of experiments performed above the freezing point of water (0 °C), molecules in a liquid state move by diffusion through the solid being dried and the phase change from liquid to gas occurs at the air-solid interface. The use of temperatures above the freezing point of water may be of great interest since the prior freezing of the sample is

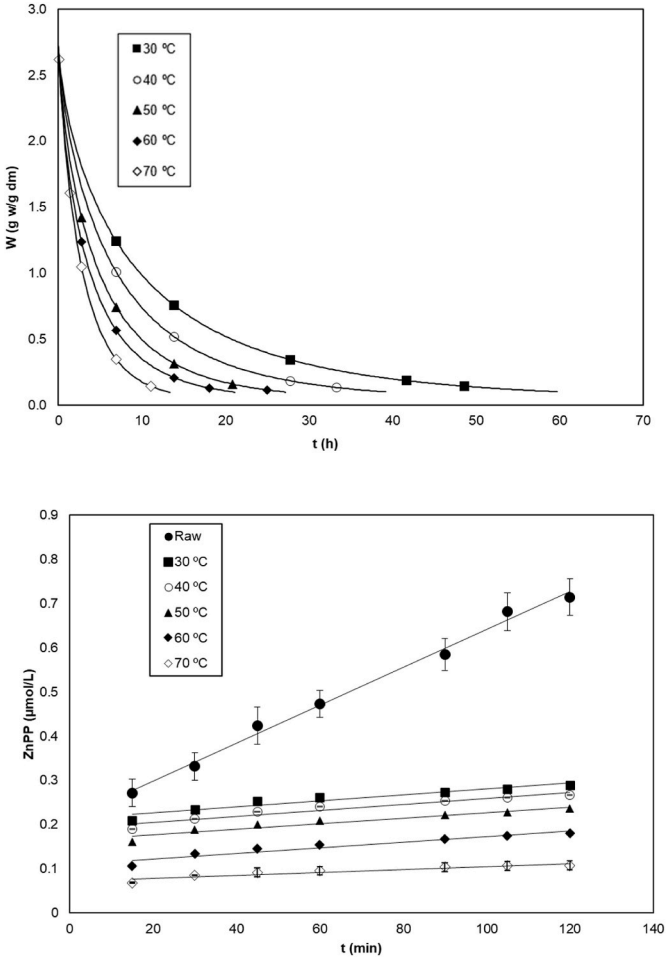

Fig. 1. Experimental and simulated (Weibull model) drying kinetics of pork liver at high temperatures (A) and the kinetics of ZnPP formation using dried and raw pork livers as sources of FeCH (B).

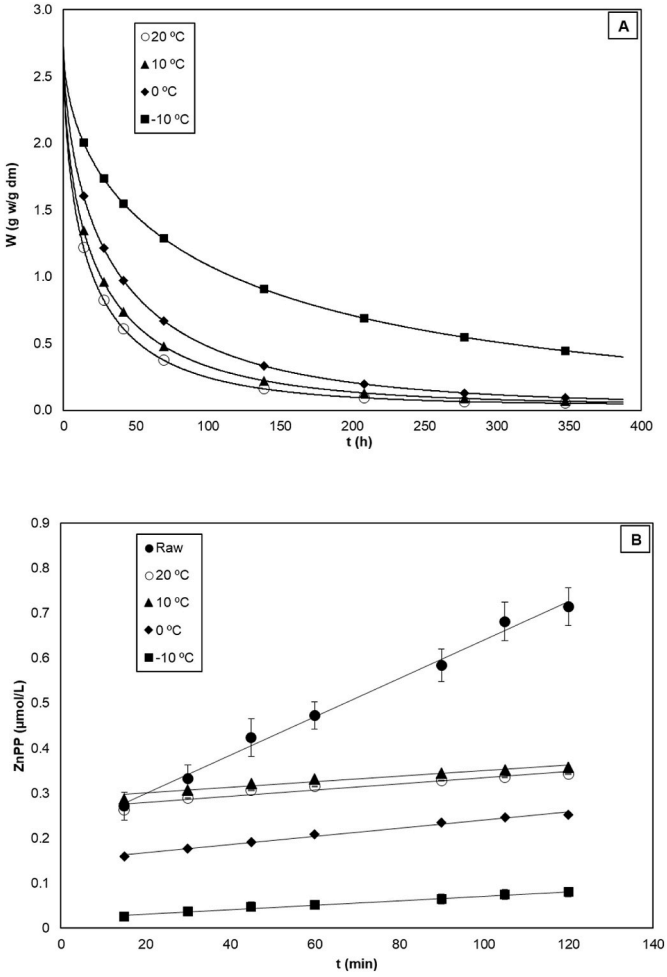

Fig. 2. Experimental and simulated (Weibull model) drying kinetics of pork liver at low temperatures (A) and the kinetics of ZnPP formation using dried and raw pork livers as sources of FeCH (B).

Table 1
Drying time and Weibull model parameters at different temperatures for the drying of pork liver.

T (°C)	t* (h)	α	β (10^3 s)	%VAR	%MRE
−10	838.8 ± 68.9	0.56 ± 0.01	402.3 ± 2.2	99.9 ± 0.1	1.00 ± 0.33
0	325.1 ± 79.2	0.61 ± 0.02	136.9 ± 4.4	99.9 ± 0.1	1.61 ± 0.94
10	225.6 ± 25.9	0.57 ± 0.01	89.2 ± 8.7	99.9 ± 0.1	1.21 ± 0.72
20	180.6 ± 55.9	0.58 ± 0.03	61.3 ± 7.5	99.9 ± 0.1	1.06 ± 0.40
30	64.5 ± 13.4	0.72 ± 0.03	33.9 ± 3.9	99.8 ± 0.1	2.39 ± 0.69
40	40.1 ± 12.1	0.76 ± 0.06	24.4 ± 2.8	99.7 ± 0.2	3.03 ± 0.66
50	38.1 ± 12.4	0.77 ± 0.03	17.1 ± 1.7	99.5 ± 0.2	4.22 ± 0.54
60	19.5 ± 8.4	0.77 ± 0.06	13.2 ± 3.7	99.3 ± 0.8	5.67 ± 1.02
70	12.1 ± 3.7	0.87 ± 0.08	10.2 ± 1.5	99.4 ± 0.7	3.28 ± 0.87

*t (h) represents the drying time needed to obtain a moisture ratio of 0.10 kg water/kg dry matter. Weibull parameters (α and β) and statistical parameters (% VAR and %MRE). For Weibull parameters, %VAR and %MRE average values ± LSD intervals are given. For t (h) average values ± SD is given.

not required. Moreover, the freezing of the sample can lead to the degradation of its internal structure brought about by the growth of ice crystals (Santacatalina et al., 2016).

Drying kinetics at different temperatures (−10, 0, 10, 20, 30, 40, 50, 60 y 70 °C) were modelled using the Weibull empirical equation (Table 1). The Weibull model allowed a satisfactory description of the drying kinetics, reporting percentages of explained variance (%VAR) of over 99%, which represents an adequate figure, particularly considering the high degree of experimental variability found in the drying of biological materials. In addition, %MRE values were lower than 10% (García-Pérez, 2007), which also indicates a reasonable fitting capability.

The figures of the α parameter showed an upward trend towards the value of 1 as the temperature increased (Fig. 3). It is worth noting that its value increased almost linearly with the temperature from 0.56 at −10 °C to 0.87 at 70 °C, obtaining intermediate values of 0.72 and 0.76 for temperatures of 30 and 40 °C, respectively (Table 1). This indicates that the drying kinetics approaches a first order kinetic progressively as the temperature rises. Therefore, it seems evident that there is a modification of the mass transfer controlling pattern as higher temperatures are used. A first order kinetic indicates that the drying rate is constant, which would mean a complete control of mass transfer by convection. This hypothesis seems consistent with the previous literature. Thus, Simal et al. (2005) used the Weibull model, also frequently known as the Page model, for the mathematical description of the drying kinetics of kiwi at different drying temperatures, from 30 to 90 °C, comparing its fitting ability with the theoretical diffusion model. It was found that as the drying temperature increased, the fitting ability of the diffusion model decreased, which denotes that moisture removal deviates from an entirely diffusion control. The temperature rise leads to an exponential increase in the diffusion rate, following an Arrhenius type relationship, leading to a rise in the amount of water on the product surface and giving more relevance to the convection, which also increases in line with the temperature but at a lower magnitude than the diffusion mechanisms. This was not observed by Simal et al. (2005) since a constant shape parameter was assumed; moreover, in the present study, a lower air velocity was used than that employed in the kiwi fruit drying kinetics modelled by Simal et al. (2005) (3 m s^{-1}) and, therefore, external transport plays an even greater role in drying kinetics.

The Weibull parameter β was affected by the drying temperature; thus, the higher the drying temperature, the lower the β figures (Machado et al., 1999). Therefore, at −10 °C a value of β of $402.3 \cdot 10^3$ s was obtained, at 20 °C one of $61.3 \cdot 10^3$ s and at 70 °C the value obtained was of $10.2 \cdot 10^3$ s (Table 1). It is complicated to compare β values with those obtained previously since they are affected by all the variables that influence the drying kinetics, such as sample geometry and mass load and distribution. The relationship of the kinetic parameter β of the Weibull model with the drying temperature followed an Arrhenius-type relationship, as observed in Fig. 4, in which it is may be seen that β departs from the linear trend marked by the rest of values at −10 °C. This indicates that below 0 °C, dehydration occurs by sublimation (Ozuna et al., 2014), while in the case of temperatures above the freezing point, water molecules are in a liquid state and are removed by evaporation (García-Pérez, 2007). The activation energy (E_a) identified at temperatures from 70 °C to 0 °C was of 29.56 ± 2.49 kJ/mol, a much lower figure than the one computed when considering only −10 and 0 °C (64.36 kJ/mol). Therefore, the process of removing water by lyophilisation consumed much more energy than in the case of evaporation. The latent heat of sublimation for pure water at −10 °C is of 51.1 kJ/mol, which represents a figure lower than the E_a identified for low temperatures (−10 and 0 °C) (Rahman et al., 2009). García-Pérez (2007) reported this difference between the E_a of evaporation and that of sublimation for the drying of cod fish, with values similar to those found in the present study on liver. Thus, an E_a of 67 kJ/mol was obtained for lyophilisation and 29.4 kJ/mol for drying at higher temperatures of cod fish (García-Pérez, 2007). Typical activation energy values lie between 12.7 and 110 kJ/mol for most of the food products (Zogzas et al., 1996; Mirzaee et al., 2009). Clemente (2003) obtained E_a values of 35.11 kJ/mol in pork meat dried at temperatures above the freezing point of water. Hii et al. (2014) reported values of between 16.3 and 22.8 kJ/mol for raw and cooked chicken meat samples, respectively, dried at 60, 70 and 80 °C. In the case of the convective drying of chicken meat, the E_a obtained was 27.85 kJ/mol (Ismail, 2017). However, in the drying kinetics of turkey breast meat samples at 60, 75 and 90 °C, a lower E_a (7.481 kJ/mol) was obtained (Elmas et al., 2020).

3.2. Kinetics of ZnPP formation from pork liver dried at different temperatures

The kinetics of ZnPP formation using dried pork liver as a FeCH source (Figs. 1B and 2B) was compared with the kinetics of ZnPP formation using raw pork liver with the aim of assessing the impact of drying on FeCH activity. The ZnPP formation kinetics from dried liver (Figs. 1B and 2B) behaved in the same way as that of the raw product, previously observed in Abril et al. (2021) with an initial burst phase followed by a steady phase at constant rate. The kinetic of ZnPP formation using raw pork liver were very similar to the one reported by Abril et al. (2021) using a larger batch in terms of both y-intercept, 0.213 ± 0.077 μM (Table 1) and 0.231 ± 0.094 μM (Abril et al., 2021), and slope (0.00428 ± 0.00011 μM/min (Table 1) and 0.0039 ± 0.0001 μM/min (Abril et al., 2021). A narrower experimental variability was found in ZnPP kinetics when using dried pork liver than when studying raw pork liver, despite the fact that the same batch was used for the

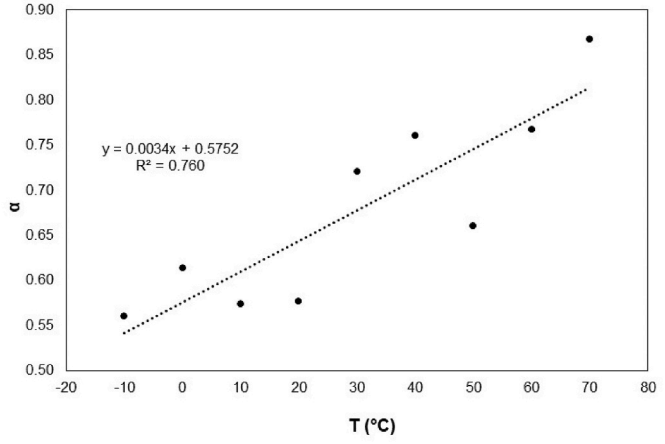

Fig. 3. Influence of the air temperature (T) on the Weibull's shape parameter (α).

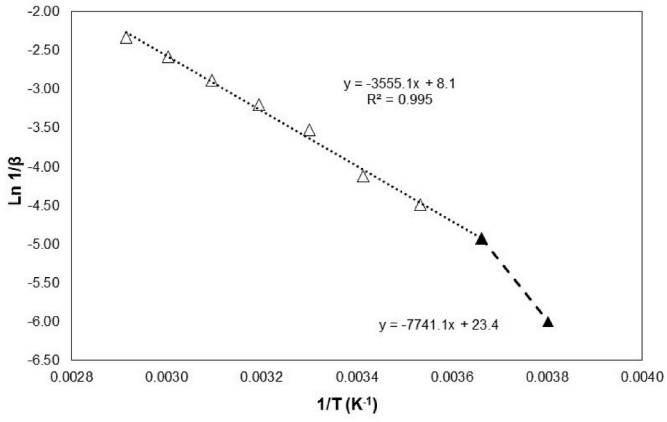

Fig. 4. Influence of the air temperature (T) on the Weibull's kinetic parameter (β).

analysis. This fact could be linked to the high enzymatic activity in the raw liver, which increases the experimental variability. Despite this fact, noticeable differences were found between the raw pork liver and the livers dried at different temperatures as FeCH sources in ZnPP formation kinetics, as depicted in Figs. 1B and 2B.

Fig. 1B shows that the apparent-FeCH concentration (EC_{app}) for samples dried at high temperatures (>20 °C) (Table 2), computed as the y-intercept of the linear relationships for the ZnPP kinetics, was dependent on the drying temperature. Thus, for the slowest drying kinetics (64.5 h to achieve 70% weight loss at 30 °C, Fig. 1A) the highest EC_{app} was achieved (0.213 μM, Fig. 5A), which gradually decreased as the drying temperature rose and, consequently, the drying time was shortened. Therefore, for liver dried at temperatures >20 °C, the higher the drying temperature, the lower the EC_{app}, which illustrates a potential thermal degradation for the FeCH enzyme. However, in the case of drying at low temperatures (≤20 °C), the opposite behaviour was found (Fig. 2B). Thus, pork livers dried at 10 °C (225.6 h) presented higher EC_{app} (0.288 μM) than those dried for longer times at 0 °C (325.1 h, 0.150 μM) and −10 °C (838.8 h, 0.021 μM). This means that a prolonged time at excessively low temperatures and the consequent exposure to oxygen leads to a loss of FeCH (Wakamatsu et al., 2007). Therefore, both drying at high temperatures for short times and drying at low temperatures for long times seem to lead to FeCH degradation and in order to better preserve the enzyme it would be more beneficial to conduct the drying process of pork liver at mild temperatures (around 10-20 °C). The EC_{app} for the ZnPP kinetics of pork liver dried at 10 and 20 °C (0.288 and 0.266 μM, respectively) was in the same order of magnitude as that of raw liver (Table 2 and Fig. 5A). This indicates that when the drying kinetics approaches room temperature, the EC_{app} was similar to raw pork liver EC_{app}, preventing the enzyme degradation found at extreme temperatures (−10 and 70 °C) (Fig. 5A). Thus, the EC_{app} for samples dried at 70 °C (0.072 μM) was very similar to that obtained for samples dried at −10 °C (0.021 mM). The protein and enzyme degradation caused by the use of excessively high or low temperatures has already been reported (Amdadul Haque et al., 2013).

Fig. 5B shows the relationship between the drying rate, calculated as the inverse of the Weibull model kinetic parameter β, and EC_{app}. The highest EC_{app} values were obtained when 1/β was between 0.01 and 0.03 (s^{-1}), obtaining values of 0.288 and 0.266 μM. However, it should be noted that the extreme values of the kinetic parameter identified at the lowest (−10 °C) and the highest temperatures (70 °C) corresponded to the lowest values of EC_{app}, 0.021 at −10 °C and 0.072 μM at 70 °C. As previously mentioned, this indicates that the extreme values of temperature, and therefore of drying rate, negatively affect EC_{app}, inducing a degradation of the initial ZnPP concentration. Therefore, temperatures close to room conditions (10 and 20 °C) denote a maximum in the EC_{app} vs 1/β figure, separating the region of low temperatures, in which the temperature rise led to an increase in both the drying rate and EC_{app}, from the high temperature range, in which the opposite behaviour was evidenced. However, in the case of the shape parameter of the Weibull model (α), no clear trend was observed with EC_{app} (Fig. 5C).

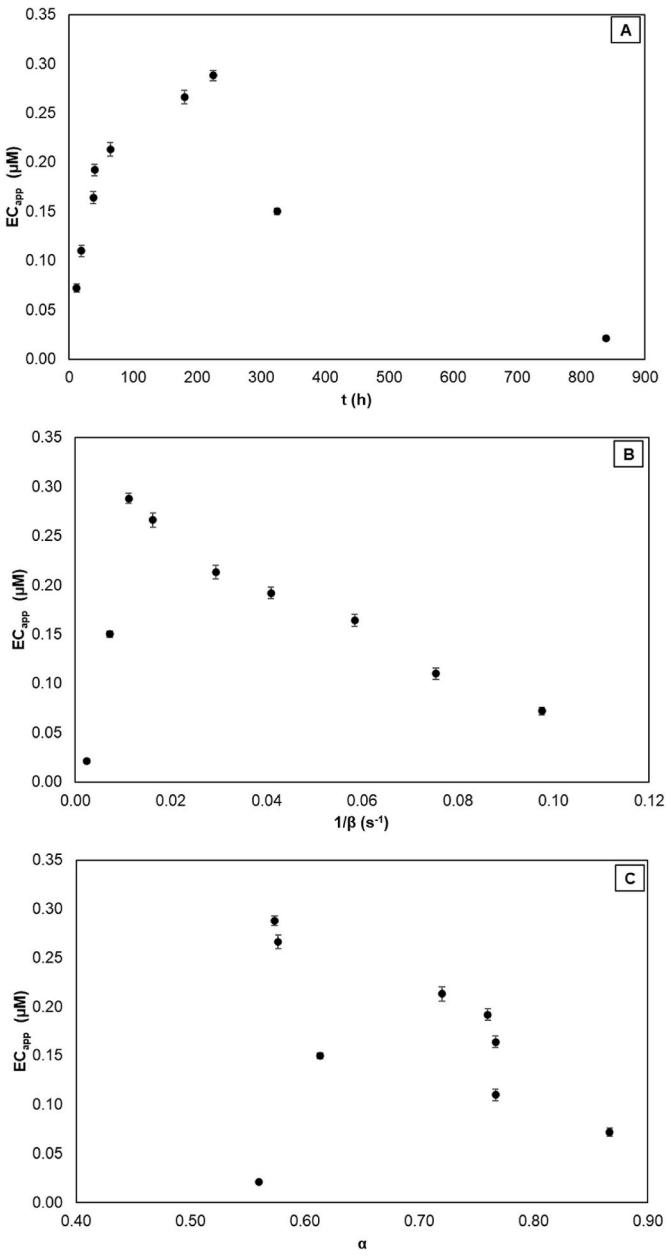

Fig. 5. Relationship between drying time and Weibull parameters with the apparent FeCH enzyme concentration (EC_{app}).

Table 2
Linear fit for the steady phase of ZnPP formation kinetics from FeCH extracts obtained from raw liver and liver dried at different temperatures.

	EC_{app} (μM)	EA (μM /min)	r	ZnPP (μM)
Raw	0.213 ± 0.077 $_{ABC}$	0.00428 ± 0.00011 $_{V}$	0.996	0.714
−10 °C	0.021 ± 0.002 $_{G}$	0.00050 ± 0.00003 $_{Y}$	0.985	0.080
0 °C	0.150 ± 0.003 $_{DEF}$	0.00091 ± 0.00005 $_{W}$	0.989	0.252
10 °C	0.288 ± 0.005 $_{A}$	0.00062 ± 0.00006 $_{XY}$	0.950	0.358
20 °C	0.266 ± 0.007 $_{AB}$	0.00068 ± 0.00009 $_{X}$	0.991	0.343
30 °C	0.213 ± 0.007 $_{ABCD}$	0.00067 ± 0.00009 $_{X}$	0.920	0.289
40 °C	0.192 ± 0.006 $_{BCD}$	0.00067 ± 0.00008 $_{X}$	0.932	0.266
50 °C	0.164 ± 0.006 $_{CDE}$	0.00062 ± 0.00008 $_{XY}$	0.924	0.236
60 °C	0.109 ± 0.006 $_{EF}$	0.00063 ± 0.00008 $_{XY}$	0.917	0.181
70 °C	0.072 ± 0.004 $_{FG}$	0.00033 ± 0.00005 $_{Z}$	0.882	0.108

Enzymatic activity (EA), apparent enzyme concentration (EC_{app}), correlation coefficient (r) and final ZnPP concentration at 120 min (ZnPP).
For EC_{app} and EA average values ± LSD intervals are given.
(A, B, C, D, E, F, G) and (V, W, X, Y, Z) show homogeneous groups established from LSD intervals ($p < 0.05$) for EC_{app} and EA, respectively.

As explained in the methodology (section 2.6.), the slope of the linear fit for the steady-state phase of ZnPP kinetics is proportional to the enzymatic activity (EA) expressed as the product formation rate. Figs. 1B and 2B illustrates the different performance of the enzyme extracted from dried and raw pork livers in terms of EA. Thus, Table 2 shows that the values of EA for the kinetics of dried pork liver ranged between 0.00033 and 0.00091 μM/min, while it was 0.00428 μM/min for raw pork liver, which represents a figure one order of magnitude higher. A statistical analysis revealed that the influence of the drying temperature on EA was statistically significant ($p < 0.05$), with the highest EA found at 0 °C (0.00091 μM/min). The lowest EA values, meanwhile, were obtained when drying was conducted at −10 and 70 °C, which presented

EA figures that were 45.1% (0.00050 μM/min at −10 °C) and 63.7% (0.00033 μM/min at 70 °C) lower than those of the liver dried at 0 °C. Between 10 and 60 °C, the EA ranged between 0.00062 and 0.00067 μM/min, and the temperature effect was negligible. This indicates that temperatures that are either excessively low (with the consequent long dehydration times) or high (with the consequent thermal degradation), cause a decrease in the catalytic activity in ZnPP formation.

There is no specific literature on the drying of pork liver and how drying affects the FeCH activity. However, there are studies that show that the FeCH, starts to reduce its activity at incubation temperatures above 40 °C (Dailey et al., 1994). While, Becker et al. (2012) postulated that at temperatures above 60 °C the ZnnPP was not formed in pork homogenates. In addition, regarding how drying affects the enzymatic activity, Perdana et al. (2012) demonstrated how enzymes are sensitive to heat and can, therefore, be inactivated during drying. In addition, Aksoy et al. (2019) and Baslar et al. (2014) demonstrated that high temperatures lead to the degradation of heat-sensitive components, such as proteins. Jaiswal et al. (2010) obtained similar results when evaluating the polyphenol oxidase (PPO) of arils from raw pomegranates dehydrated at 100 °C, obtaining a 68% decrease in their activity (647.7 units/mL in raw arils compared to 205.7 units/mL in dry arils). Similarly, Parra Vergara (2013) observed an 89.5% decrease in the enzymatic activity of peroxidase in dehydrated broccoli at 75 °C, compared to fresh broccoli. In addition, Maca et al. (2013) showed that the use of high drying temperatures influences the enzymatic activity of pectin-methylesterase in Tree Tomatoes (*Solanum betaceum*) and reported a 28% decrease in the product concentration by increasing the drying temperature from 60 °C to 90 °C. Meanwhile, Shofian et al. (2011) highlighted that the freeze-drying process in tropical fruits, such as mango, papaya and carambola, accelerated the enzymatic reactions involved in the browning generated by polyphenoloxidases (PPO). In freeze-dried tomatoes, cell walls were shown to be altered, triggering the release of oxidative enzymes that destroyed antioxidant compounds in the fruit (Chang et al., 2006). In the present study, low temperatures (−10 °C and 0 °C) had a detrimental effect on EC_{app}, compared to drying temperatures close to room temperature (10 °C and 20 °C) which provided a similar EC_{app} to that of raw pork liver (0.213 μM). In the case of pork liver dried at 10 and 20 °C, the EA was significantly reduced (0.00062 and 0.00068 μM/min) compared to that of raw pork liver (0.00428 μM/min), possibly due to conformational changes in the protein structure of the enzyme (Oyinloye & Yoon, 2020).

4. Conclusions

Air drying has been proven to be an effective method to stabilise the pork liver and obtain a FeCH extract that can be used for ZnPP formation so it can be stored for a longer time at a moderate cost. However, it should be noted that drying significantly affects both the apparent-FeCH concentration and activity. Thus, high drying temperatures (>30 °C), and low drying temperatures (<0 °C), cause significant changes ($p < 0.05$) in the concentration of FeCH as well as in its subsequent activity, both of which were completely dependent on the drying temperature. Drying conditions close to room temperature (between 10 and 20 °C) were the most adequate conditions considering both apparent-FeCH concentration and activity. Further research should elucidate how drying affects the structure of FeCH, which would contribute to an understanding of the observed phenomena on its catalytic activity for ZnPP formation, as well as any further industrial application. In addition, it could be a relevant matter to gain insight into the use of drying techniques that minimise or avoid exposure to oxygen, such as vacuum drying or freeze drying. Two different applications of the dried pork liver as FeCH source could be envisioned: i) its incorporation to raw-cured products, such as salami, fuet or sausage, to induce the formation of ZnPP during curing and ii) the industrial production of ZnPP as a natural colorant for the food industry.

CRediT authorship contribution statement

B. Abril: Methodology, Formal analysis, Investigation, Writing – original draft. **E.A. Sanchez-Torres:** Methodology, Formal analysis. **R. Bou:** Conceptualization, Methodology, Writing – review & editing. **J. Benedito:** Formal analysis, Writing – review & editing, Supervision, Project administration, Funding acquisition. **Jose V. Garcia-Perez:** Conceptualization, Methodology, Writing – review & editing, Supervision.

Declaration of competing interest

The authors declare that they have no known competing financial interests or personal relationships that could have appeared to influence the work reported in this paper.

Data availability

Data will be made available on request.

Acknowledgements

The authors acknowledge the financial support from the “Ministerio de Economía y Competitividad (MINECO)” and “Instituto Nacional de Investigación y Tecnología Agraria y Alimentaria (INIA)” in Spain (Projects RTA2017-00024-C04-03 and RTA2017-00024-C04-01).

References

Abril, B., Sánchez-Torres, E. A., Bou, R., García-Pérez, J. V., & Benedito, J. (2021). Ultrasound intensification of Ferrochelatase extraction from pork liver as a strategy to improve ZINC-protoporphyrin formation. *Ultrasonics Sonochemistry, 78*, Article 105703. https://doi.org/10.1016/j.ultsonch.2021.105703

Adamsen, C. E., Møller, J. K., Hismani, R., & Skibsted, L. H. (2004). Thermal and photochemical degradation of myoglobin pigments in relation to colour stability of sliced dry-cured Parma ham and sliced dry-cured ham produced with nitrite salt. *European Food Research and Technology, 218*(5), 403–409. https://doi.org/10.1007/s00217-004-0891-8

Aksoy, A., Karasu, S., Akcicek, A., & Kayacan, S. (2019). Effects of different drying methods on drying kinetics, microstructure, color, and the rehydration ratio of minced meat. *Foods, 8*(6), 216. https://doi.org/10.3390/foods8060216

Amdadul Haque, M., Putranto, A., Aldred, P., Chen, J., & Adhikari, B. (2013). Drying and denaturation kinetics of whey protein isolate (WPI) during convective air drying process. *Drying Technology, 31*(13–14), 1532–1544. https://doi.org/10.1080/07373937.2013.794832

AOAC. (1997). Official methods 950.46. In *Official methods of analysis* (16th ed.).

Baque, M., Macías, B., & Cornejo, F. (2010). *Influencia de pre tratamientos convencionales en el proceso de secado de manzana y en las características físicas del producto final. Escuela Superior Politecnica del Litoral, Guayaquil.* http://www.dspace.espol.edu.ec/handle/123456789/8993.

Başlar, M., Kılıçlı, M., Toker, O. S., Sağdıç, O., & Arici, M. (2014). Ultrasonic vacuum drying technique as a novel process for shortening the drying period for beef and chicken meats. *Innovative Food Science & Emerging Technologies, 26*, 182–190. https://doi.org/10.1016/j.ifset.2014.06.008

Becker, E. M., Westermann, S., Hansson, M., & Skibsted, L. H. (2012). Parallel enzymatic and non-enzymatic formation of zinc protoporphyrin IX in pork. *Food Chemistry, 130*(4), 832–840. https://doi.org/10.1016/j.foodchem.2011.07.090

Buzrul, S. (2022). Reassessment of thin-layer drying models for foods: A critical short communication. *Processes, 10*(1), 118. https://doi.org/10.3390/pr10010118

Chang, C. H., Lin, H. Y., Chang, C. Y., & Liu, Y. C. (2006). Comparisons on the antioxidant properties of fresh, freeze-dried and hot-air-dried tomatoes. *Journal of Food Engineering, 77*(3), 478–485. https://doi.org/10.1016/j.jfoodeng.2005.06.061

Chau, T. T., Ishigaki, M., Kataoka, T., & Taketani, S. (2010). Porcine ferrochelatase: The relationship between iron-removal reaction and the conversion of heme to Zn-protoporphyrin. *Bioscience, Biotechnology, and Biochemistry, 74*(7), 1415–1420. https://doi.org/10.1271/bbb.100078

Chau, T. T., Ishigaki, M., Kataoka, T., & Taketani, S. (2011). Ferrochelatase catalyzes the formation of Zn-protoporphyrin of dry-cured ham via the conversion reaction from heme in meat. *Journal of Agricultural and Food Chemistry, 59*(22), 12238–12245. https://doi.org/10.1021/jf203145p

Clemente Polo, G. (2003). *Efecto de la contracción en la cinética de secado de músculos de jamón. Tesis doctoral.* Valencia, España: Universidad Politécnica de Valencia.

Cunha, L. M., Oliveira, F. A. R., & Oliveira, J. C. (1998). Optimal experimental design for estimating the kinetic parameters of processes described by the Weibull probability distribution function. *Journal of Food Engineering, 37*, 175–191. https://doi.org/10.1016/S0260-8774(98)00085-5

Dailey, H. A., Sellers, V. M., & Dailey, T. A. (1994). Mammalian ferrochelatase. Expression and characterization of normal and two human protoporphyric ferrochelatases. *Journal of Biological Chemistry, 269*(1), 390–395.

Echegaray, N., Gómez, B., Barba, F. J., Franco, D., Estévez, M., Carballo, J., … Lorenzo, J. M. (2018). Chestnuts and by-products as source of natural antioxidants in meat and meat products: A review. *Trends in Food Science & Technology, 82*, 110–121. https://doi.org/10.1016/j.tifs.2018.10.005

EFPRA. (2021). *Rendering in numbers*. https://efpra.eu/wp-content/uploads/2021/07/Rendering-in-numbers-Infographic.pdf. (Accessed 16 May 2022) Accessed on.

Elmas, F., Bodruk, A., Köprüalan, Ö., Arıkaya, Ş., Koca, N., Serdaroğlu, F. M., … Koc, M. (2020). Drying kinetics behavior of Turkey breast meat in different drying methods. *Journal of Food Process Engineering, 43*(10), Article e13487. https://doi.org/10.1111/jfpe.13487

Estévez, M., Morcuende, D., Ramırez, R., Ventanas, J., & Cava, R. (2004). Extensively reared Iberian pigs versus intensively reared white pigs for the manufacture of liver pâté. *Meat Science, 67*(3), 453–461. https://doi.org/10.1016/j.meatsci.2003.11.019

García-Pérez, J. V. (2007). *Contribución Al estudio de La aplicación de ultrasonidos de potencia en el secado convectivo de alimentos. Tesis doctoral*. Universidad Politécnica de Valencia.

Garcia-Perez, J. V., Carcel, J. A., Riera, E., Rosselló, C., & Mulet, A. (2012). Intensification of low-temperature drying by using ultrasound. *Drying Technology, 30*(11–12), 1199–1208. https://doi.org/10.1080/07373937.2012.675533

García-Pérez, J. V., Ozuna, C., Ortuño, C., Cárcel, J. A., & Mulet, A. (2011). Modeling ultrasonically assisted convective drying of eggplant. *Drying Technology, 29*(13), 1499–1509. https://doi.org/10.1080/07373937.2011.576321

Guiné, R. (2018). The drying of foods and its effect on the physical-chemical, sensorial and nutritional properties. *International Journal of Food Engineering, 2*(4), 93–100. https://doi.org/10.18178/ijfe.4.2.93-100

Hii, C. L., Itam, C. E., & Ong, S. P. (2014). Convective air drying of raw and cooked chicken meats. *Drying Technology, 32*(11), 1304–1309. https://doi.org/10.1080/07373937.2014.924133

Ismail, O. (2017). An experimental and modeling investigation on drying of chicken meat in convective dryer. *Studia Universitatis Babes-Bolyai, Chemia, 62*(4), 459–469. https://doi.org/10.24193/subbchem.2017.4.3

Jaiswal, V., DerMarderosian, A., & Porter, J. R. (2010). Anthocyanins and polyphenol oxidase from dried arils of pomegranate (Punica granatum L.). *Food Chemistry, 118*(1), 11–16. https://doi.org/10.1016/j.foodchem.2009.01.095

Kuddus, M. (2019). Introduction to food enzymes. In *Enzymes in food biotechnology* (pp. 1–18). Academic Press. https://doi.org/10.1016/B978-0-12-813280-7.00001-3.

Maca, M. P., Osorio, O., & Mejía-España, D. F. (2013). Inactivación térmica de pectinmetilesterasa en tomate de árbol (Solanum betaceum). *Informacion Tecnologica, 24*(3), 41–50. https://doi.org/10.4067/S0718-07642013000300006

Machado, M. F., Oliveira, F. A., & Cunha, L. M. (1999). Effect of milk fat and total solids concentration on the kinetics of moisture uptake by ready-to-eat breakfast cereal. *International Journal of Food Science and Technology, 34*(1), 47–57. https://doi.org/10.1046/j.1365-2621.1999.00238.x

Meziane, S. (2011). Drying kinetics of olive pomace in a fluidized bed dryer. *Energy Conversion and Management, 52*(3), 1644–1649. https://doi.org/10.1016/j.enconman.2010.10.027

Mirzaee, E., Rafiee, S., Keyhani, A., & Emam-Djomeh, Z. (2009). Determining of moisture diffusivity and activation energy in drying of apricots. *Research in Agricultural Engineering, 55*(3), 114–120.

Morita, H., Niu, J., Sakata, R., & Nagata, Y. (1996). Red pigment of Parma ham and bacterial influence on its formation. *Journal of Food Science, 61*, 1021–1023. https://doi.org/10.1111/j.1365-2621.1996.tb10924.x

Oyinloye, T. M., & Yoon, W. B. (2020). Effect of freeze-drying on quality and grinding process of food produce: A review. *Processes, 8*(3), 354. https://doi.org/10.3390/pr8030354

Ozuna, C., Cárcel, J. A., Walde, P. M., & Garcia-Perez, J. V. (2014). Low temperature drying of salted cod (Gadus morhua) assisted by high power ultrasound: Kinetics and physical properties. *Innovative Food Science & Emerging Technologies, 23*, 146–155. https://doi.org/10.1016/j.ifset.2014.03.008

Parra Vergara, J. C. (2013). *Determinación de la cinética de liofilización en floretes de brócoli (Brassica oleracea L, var. Legacy) y evaluación del contenido de ácido L-ascórbico (L-AA) y actividad peroxidasa (POD)*. Duitama: Universidad Nacional Abierta y a Distancia.

Perdana, J., Fox, M. B., Schutyser, M. A. I., & Boom, R. M. (2012). Enzyme inactivation kinetics: Coupled effects of temperature and moisture content. *Food Chemistry, 133*(1), 116–123. https://doi.org/10.1016/j.foodchem.2011.12.080

Praestgaard, E., Elmerdahl, J., Murphy, L., Nymand, S., McFarland, K. C., Borch, K., & Westh, P. (2011). A kinetic model for the burst phase of processive cellulases. *FEBS Journal, 278*(9), 1547–1560. https://doi.org/10.1111/j.1742-4658.2011.08078.x

Rahman, M. S., Machado-Velasco, M., Sosa-Morales, M. E., & Velez-Ruiz, J. F. (2009). Freezing point: Measurement, data, and prediction. *Food Properties Handbook, 2*, 153–192.

Roy, I., & Gupta, M. N. (2004). Freeze-drying of proteins: Some emerging concerns. *Biotechnology and Applied Biochemistry, 39*(2), 165–177. https://doi.org/10.1042/BA20030133

Sánchez-Torres, E. A., Abril, B., Benedito, J., Bon, J., & García-Pérez, J. V. (2021). Water desorption isotherms of pork liver and thermodynamic properties. *LWT, 149*, Article 111857. https://doi.org/10.1016/j.lwt.2021.111857

Santacatalina, J. V., Contreras, M., Simal, S., Cárcel, J. A., & Garcia-Perez, J. V. (2016). Impact of applied ultrasonic power on the low temperature drying of apple. *Ultrasonics Sonochemistry, 28*, 100–109. https://doi.org/10.1016/j.ultsonch.2015.06.027

Santacatalina, J. V., Ozuna, C., Cárcel, J. A., Garcia-Perez, J. V., & Mulet, A. (2011). Quality assessment of dried eggplant using different drying methods: Hot air drying, vacuum freeze drying and atmospheric freeze drying. In *Proceedings of the 11th international congress on engineering and food*.

Santacatalina, J. V., Rodríguez, O., Simal, S., Cárcel, J. A., Mulet, A., & García-Pérez, J. V. (2014). Ultrasonically enhanced low-temperature drying of apple: Influence on drying kinetics and antioxidant potential. *Journal of Food Engineering, 138*, 35–44. https://doi.org/10.1016/j.jfoodeng.2014.04.003

Sassa, A., Beard, W. A., Shock, D. D., & Wilson, S. H. (2013). Steady-state, pre-steady-state, and single-turnover kinetic measurement for DNA glycosylase activity. *Journal of Visualized Experiments*, (78), Article e50695. https://doi.org/10.3791/50695

Shofian, N. M., Hamid, A. A., Osman, A., Saari, N., Anwar, F., Pak Dek, M. S., & Hairuddin, M. R. (2011). Effect of freeze-drying on the antioxidant compounds and antioxidant activity of selected tropical fruits. *International Journal of Molecular Sciences, 12*(7), 4678–4692. https://doi.org/10.3390/ijms12074678

Simal, S., Femenia, A., Garau, M. C., & Rosselló, C. (2005). Use of exponential, Page's and diffusional models to simulate the drying kinetics of kiwi fruit. *Journal of Food Engineering, 66*(3), 323–328. https://doi.org/10.1016/j.jfoodeng.2004.03.025

Taketani, S., & Tokunaga, R. (1982). Purification and substrate specificity of bovine liver-ferrochelatase. *European Journal of Biochemistry, 127*(3), 443–447. https://doi.org/10.1111/j.1432-1033.1982.tb06892.x

Wakamatsu, J. I., Murakami, N., & Nishimura, T. (2015). A comparative study of zinc protoporphyrin IX-forming properties of animal by-products as sources for improving the color of meat products. *Animal Science Journal, 86*(5), 547–552. https://doi.org/10.1111/asj.12326

Wakamatsu, J., Nishimura, T., & Hattori, A. (2004a). A Zn–porphyrin complex contributes to bright red color in Parma ham. *Meat Science, 67*(1), 95–100. https://doi.org/10.1016/j.meatsci.2003.09.012

Wakamatsu, J. I., Okui, J., Hayashi, N., Nishimura, T., & Hattori, A. (2007). Zn protoporphyrin IX is formed not from heme but from protoporphyrin IX. *Meat Science, 77*(4), 580–586. https://doi.org/10.1016/j.meatsci.2007.05.008

Wakamatsu, J., Okui, J., Ikeda, Y., Nishimura, T., & Hattori, A. (2004b). Establishment of a model experiment system to elucidate the mechanism by which Zn–protoporphyrin IX is formed in nitrite-free dry-cured ham. *Meat Science, 68*(2), 313–317. https://doi.org/10.1016/j.meatsci.2004.03.014

Zogzas, N. P., Maroulis, Z. B., & Marinos-Kouris, D. (1996). Moisture diffusivity data compilation in foodstuffs. *Drying Technology, 14*(10), 2225–2253. https://doi.org/10.1080/07373939608917205